Steel and Composite Structures, *Vol. 15, No. 4 (2013) 425-438*
DOI: http://dx.doi.org/10.12989/scs.2013.15.4.425

Experimental research on sagging bending resistance of steel sheeting-styrofoam-concrete composite sandwich slabs

P.Z. Cao*, Y.F. Lu [a] and Kai Wu [b]

College of Civil and Transportation Engineering, Hohai University, Nanjing, Jiangsu, P.R. China

(Received March 01, 2012, Revised July 16, 2013, Accepted August 01, 2013)

Abstract. A new-styrofoam-concrete composite sandwich slab with function of heat insulation is designed. Four full-scale simply supported composite sandwich slabs with different shear connectors are tested. Parameters under study are the thickness of the concrete, the height of profiled steel sheeting, the influence of shear connectors including the steel bars and self-drilling screws. Experimental results showing that four specimens mainly failed in bending failure mode; the shear connectors can limit the longitudinal slippery between the steel profiled sheeting and the concrete effectively and thus guarantee the good composite action and cooperative behavior of two materials. The ultimate sagging bending resistance can be determined based on plastic theory. This new composite sandwich slab has high sagging bending resistance and good ductility. Additionally, these test results help the design and application of this new type of composite sandwich slab.

Keywords: composite sandwich slabs; re-entrant trough profiled steel sheeting; shear connectors; bending-bearing capacities; experimental research; bending failure

1. Introduction

Normal composite slabs comprised of cold-formed steel with profiled sheeting and structural concrete take advantages of the tensile strength of steel and compressive strength of concrete, and have the merits of high rigidity, good ductility, easy and quick installation, and low cost. Composite slabs (Johnson and Buckby 2004) have been widely used in multi-storied and high-rise steel framed constructions over the last two decades. Schuster and Ekberg (1970) and proposed the ultimate bending strength design method and provided semi-theoretical and semi-empirical equations for the ultimate bearing capacity of composite slabs. Porter and Ekberg (1976) at Iowa State University reported that the longitudinal shear resistance of the composite slabs could be calculated via the m-k method on the basis of performance tests. However, the engineering designers currently calculate the bearing capacity of the composite slab floor system in the live load as reinforced concrete slabs and usually view profiled steel sheeting as forms, because the only indentation and embossments in the profiled sheeting cannot provide a satisfied longitudinal

*Corresponding author, Professor, E-mail: pzcao@hhu.edu.cn
[a] Student, E-mail: shyboy_2000@ 126.com
[b] Ph.D., E-mail: wukai19811240@163.com

http://www.techno-press.org/?journal=scs&subpage=8 ISSN: 1229-9367 (Print), 1598-6233 (Online)

shear resistance. Hence, several literatures cover that many new shear connectors have been studied, which may strengthen the cooperation of two materials. Shear resistance and structural response of perfobond-rib and T-shape perfobond shear connectors with various geometry configuration have been experimentally researched by Kim and Jeong (2010), Ahn *et al*. (2010) and Vianna *et al*. (2008, 2009). And the capacity of channel shear connectors embedded in concrete have been investigated by virtue of push-out tests (Maleki and Bagheri 2008a, 2008b and Maleki and Mahoutian 2009). What's more, de Anderade *et al*. (2004) noted the enhancement of the horizontal shear interaction at the open trough profiled steel sheeting-concrete interface of composite slabs with the adoption of shear screws. Test results demonstrated that the settlement of the self-drilling screws could improve the load carrying capacity and ductility of the composite slabs. However, most of literatures focused on the shear connectors welded onto steel beams or beam-columns. Additionally, there is little information concerned about the shear connectors set onto the profiled steel sheeting and previous studies failed to provide the detailed calculation method for the sagging bending resistance of a composite slab with shear screws.

This paper proposes an innovative composite slab system – a re-entrant trough profiled steel sheeting-styrofoam-concrete composite sandwich slab. It was constructed by embedding the styrofoam plate into the troughs of the steel sheeting to replace the concrete as the insulating layer. Then shear connectors were attached to the flanges of the steel sheeting. Finally, the concrete was cast. The dead weight of the new composite slab is lighter than the normal one and meanwhile its thermal insulating performance is better. The purpose of this paper is to clarify the sagging bending resistance of this new composite sandwich slab and provide the technical basis for its design and applications.

2. Test specimen fabrication

A total of 4 re-entrant trough profiled steel sheeting- styrofoam-concrete composite sandwich slabs were built and studied by the two point bending tests in order to access the sagging bending resistance. The number and geometric size of the test specimens are given in Table 1. The concrete mix of C30 grade, designed as per the relevant Chinese Standard (2000), and the steel profiled sheeting based on Q235 grade steel are used. Steel reinforcing bar meshes (using 4 mm diameter bars) with the space of 150 mm in both directions were placed in the upper concrete in order to avoid formation of shrinkage cracks and temperature cracks. It is assumed that the shear connectors are totally subject to the longitudinal shear force between the profiled steel sheeting and the concrete, and that the bond strength at the contact interface between them is negligible. The shear connectors were designed by virtue of elastic method referred to the design theory of composite beams. The longitudinal shear force at the interface is calculated based on the transformed section method. The total number of shear connectors can be derived by dividing the longitudinal shear force by the single shear capacity of each shear connector. According to the result of calculation, the self-drilling screws slanted through the top flange of profiled steel sheeting of BBZ-1, BBZ-2 and BBZ-3 and their effective anchorage length in the upper concrete is 20 mm. The shear steel bars (HRB400 level) of 6 mm diameter were soldered to the top flanges in the BBJ-1. The 32 mm thick styrofoam plates were set in the troughs of the profiled steel sheeting to substitute for the concrete in the tensile zone. Subsequently, the concrete layer was casted. Fig. 1 shows the internal structure of the composite sandwich slabs.

The concrete used for the casting is of C30 grade. The mean average 28-day cube strength of

the concrete under compression is listed in Table 1, by testing cube specimens (three from every slab). The BD65-555-185 re-entrant trough profiled steel sheeting is adopted in these tests. Its geometric shape is shown in Fig. 2 and the parameters of its cross section and its mechanical property is listed in Table 2. The self-drilling screw details are illustrated in Fig. 3 and in Table 3. Yielding strength and ultimate tensile strength of shear steel bars is 440 MPa and 605 MPa respectively.

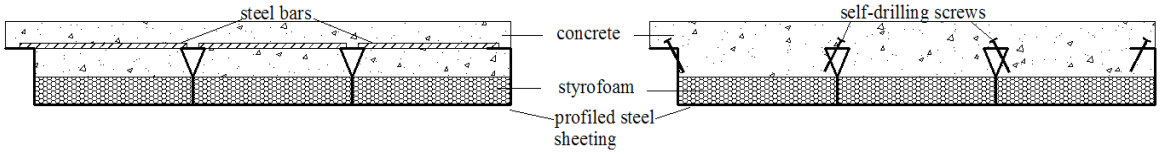

(a) Specimen with shear bars (b) Specimen with shear screws

Fig. 1 Cross-section view of the internal structure of a composite sandwich slab

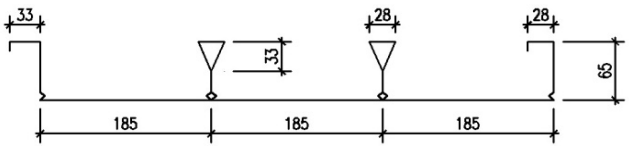

Fig. 2 Geometric Shape of BD65-555-185

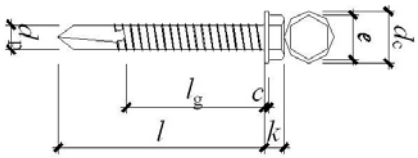

Fig. 3 Self-drilling screw details

Table 1 Group of the test specimens

No.	Span	Width	Designed thickness	Measured thickness	Conc.Comp. strength f_c	Conc. thickness	Shear span L_s	n_1*	n_2	n_3	n_4
	/mm	/mm	/mm	/mm	/MPa	/mm	/mm				
BBZ-1	2400	555	85	87	26.7	55	600	25	25	None	None
BBZ-2			95	96	24.5	64	600	38	38	None	None
BBZ-3			115	108	22.6	76	600	43	43	None	None
BBJ-1			95	97	22.4	65	600	None	None	18	7

n_1* is total number of the screws lied in the shear span; n_2 is total number of the screws lied in the pure bending span; n_3 is total number of the steel bars lied in the shear span; n_4 is total number of the steel bars lied in the pure bending span

Table 2 Geometry and strength of profiled sheeting

Area A_p	Moment of inertia I_x	Section factor W_x	X_o	Thickness t	Yielding strength f_y	Tensile strength f_u	Elastic modulus E
/mm^2	/mm^4	/mm^3	/mm	/mm	/MPa	/MPa	$\times 10^5$MPa
952	477030	10097	47	0.8	213	317	2.06

Table 3 Parameters of self drilling screw

d_c/mm	d_p/mm	e/mm	c/mm	k/mm	l/mm	l_g/mm	f_y/MPa
8.8	4.2	7.59	0.8	3.6	50	38	320

3. Test setup

Load was applied by a 250 kN hydraulic ram, which was jacked against the reaction frame. The load was distributed onto the slab as two line loads through a spreader beam system. The specimens were supported by pin and roller type supports with an overhang of 50 mm at both ends. The detailed and schematic views of the test setup are shown in Figs. 4-5 respectively. The load was applied under hybrid load-displacement control. Specifically, it was under load control before the concrete cracking and then under displacement control after the concrete cracking. In the beginning, load increment under load control for each level was 15% of the theoretical calculated results based on the current code and each level lasted 3 minutes. After the concrete cracking, displacement increment of the mid span for each level is 3 mm, which was applied to the test specimens until failure.

The relative slip between the interface of the profiled steel sheeting and the concrete at the end of slabs were measured by dial gauges (ranging from 0 mm to 10 mm). The deflections of the mid-span and 1/4-span and deformations at the support were measured by Linear Variable Differential Transformers (LVDTs). LVDTs were connected to the TS-3890. Data were automatically recorded at each load level. The setup of the LVDTs is shown in Fig. 5. The strain

Fig. 4 Optical image of test setup for composite sandwich slabs

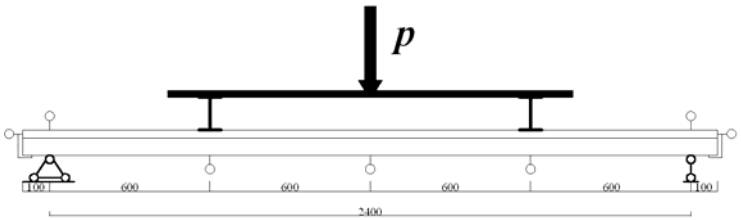

Fig. 5 Loading arrangement on the slab

Fig. 6 Arrangement of strain gauges on slabs

gauges were adhered to the steel profiled sheeting positioned in the mid-span, 1/4-span loading point, 1/8-span, and the concrete surface positioned at the mid-span, as is shown in Fig. 6. All data in the whole loading history were automatically recorded using TS-3890.

4. Test results and analysis

4.1 Test phenomena

The failure modes of 3 slabs were similar. In the beginning of the tests, there were no concrete cracks or end slips. When the load amounted to about 50% P_{max} (P_{max} was the ultimate failure load), sound and slight end slip were observed due to the separation of the steel deck and the concrete. As the load gradually increased, several vertical cracks were observed near the loading point with slight sound occurring all the time. When the load reached the ultimate load carrying capacity of the slabs, the concrete crushed into pieces and steel deck suffered buckling failure at the loading point. It is shown to be the flexural failure mode (Fig. 7). The maximum end slip reached 0.6 mm among these slabs. Hence, the small slip between the interface of profiled steel sheeting and the concrete can be ignored when calculating the sagging bending resistance.

Fig. 7 Failure of the test specimen

For the specimen BBJ-1, as the load amounted to 65% P_{max}, the longitudinal cracks at the support were observed and extended readily to the loading point. When the load reached the failure load, BBJ-1 showed the same failure phenomena like above tests, where the concrete crushed into pieces, and that the steel deck suffered buckling failure near the line load. It is shown to be bending-shear failure mode. The maximum end slip reached 1.08 mm.

4.2 Analysis of the test results

The loading history, in the form of load versus slab mid-span deflection, for each test is shown in Fig. 8. The graphs of load versus strain at the bottom of the steel deck positioned at the mid-span and two loading points are shown in Fig. 9 (The strains correspond to strain gauge #7, #12, and #17, respectively.) .The graphs of load versus strain positioned on the upper flange of the steel deck and the surface of the concrete slabs at the mid span are shown in Figs. 10-11. The load-slip curves are shown in Fig. 12. In Table 4, P_{cr} is the load when the initial end slip was observed; P_{max} is the failure load and δ, s_{max} are the mid-deflections and end slips respectively when the slabs failed; $P_{L/250}$, $M_{L/250}$ are the concentrated force and its corresponding mid-span moment when the mid-deflection reaches $L/250$ (referred to the deflection limit of *EuroCode4*).

As is shown in Fig. 8, under the serviceability limit stage ($\delta \leq L/250$), load reached about 50% of the ultimate load carrying capacity and the load has a basically linear correlation with the deflection. Advanced composite action and cooperation between the steel sheeting and the concrete has been achieved. As the load increased, the slight slips at the end support and the concrete cracks between the steel deck ribs were observed. Then, the behaviors of composite sandwich slabs came into the inelastic stage. The load-deflection curves tended to slow down and the mid-span deflections increased drastically with a small increase in the loads. Specifically, the slabs including BBZ-2 and BBZ-3, with slow development of the concrete cracks, kept a high flexural rigidity and good ductility. However, for BBZ-1 and BBJ-1, the loads dropped readily when the loads amounted to ultimate load carrying capacity, mainly because the shear screws could not provide sufficient anti-uplift force in the shear span to avoid the vertical separation of the steel deck-to-concrete interface. The deflection δ of the composite slabs under service loads does not exceed the limit $L/250$ based on the regulation of *EuroCode4*. According to the test

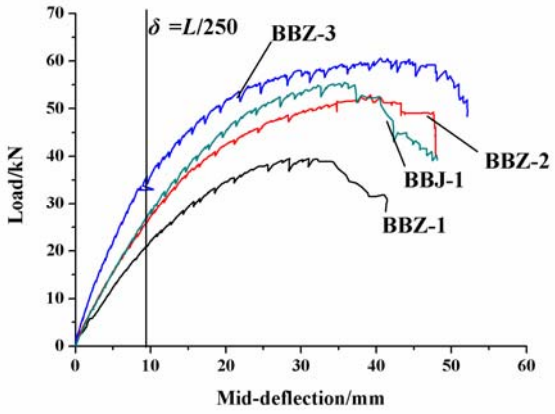

Fig. 8 Load- deflection curves of the composite sandwich slabs

Table 4 Test result of the composite sandwich slabs

No.	Occurrence of end slips			Deflection $\delta = L/250$		Maximum test loads			
	P_{cr}	M_{cr}	s	$P_{L/250}$	$M_{L/250}$	P_{max}	M_{max}	δ	s_{max}
	kN	kN·m	mm	kN	kN	kN	kN·m	mm	mm
BBZ-1	26.35	7.91	0.04	21.23	6.37	39.53	11.86	28.49	1.08
BBZ-2	32.15	9.65	0.07	26.28	7.88	52.88	15.86	39.22	0.31
BBZ-3	30.15	9.05	0.08	34.43	10.33	60.58	18.17	42.66	0.60
BBJ-1	28.38	8.51	0.24	27.55	8.27	55.55	16.67	36.3	0.25

results, the slabs had large deformation. Thus, this paper suggests the above code as the central deflection limit. In the tests the maximum central deflection, reaching $L/80$ under the failure load, far exceeded the deflection limit, which proves that the slabs have good ductility.

As is shown in Fig. 9, when the load reached the ultimate load carrying capacity, the strains at the two loading points were larger than the values of the mid span, and the former reached the yielding strain (about 1050×10^{-6}) prior to the latter, because the loading points underwent interaction of maximum moment and shear force while the mid-span only suffered with pure moment. As is shown in Figs. 10-11, the upper flange of the mid-span steel deck was under tensile stress. The results indicated that neutral axis of the mid-span was located above the upper flange of

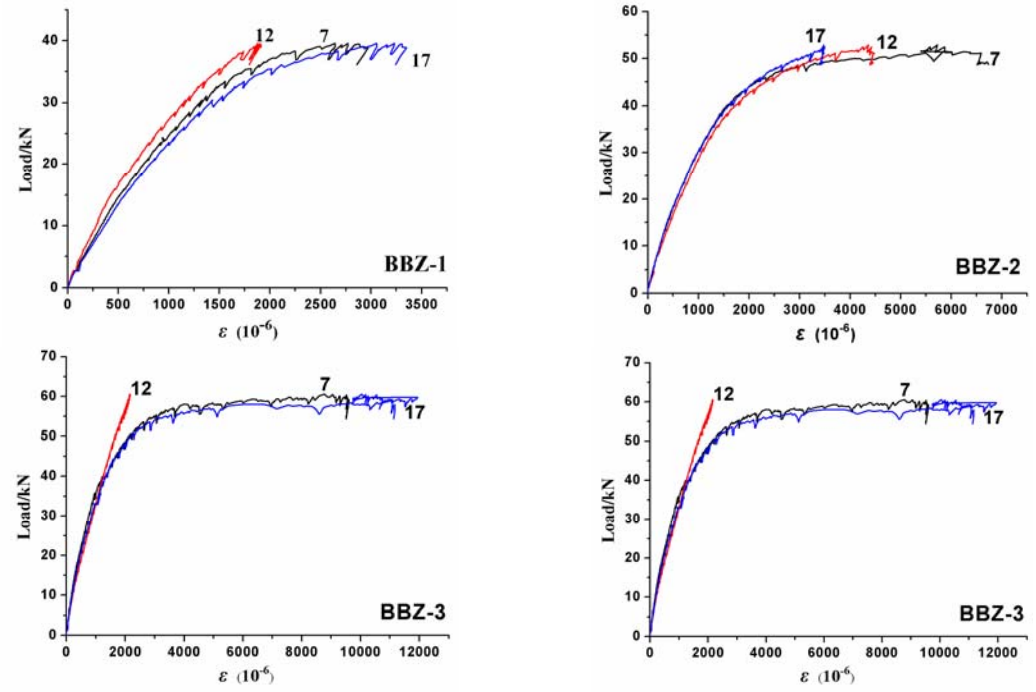

Fig. 9 Load-strain on the bottom of the steel sheet

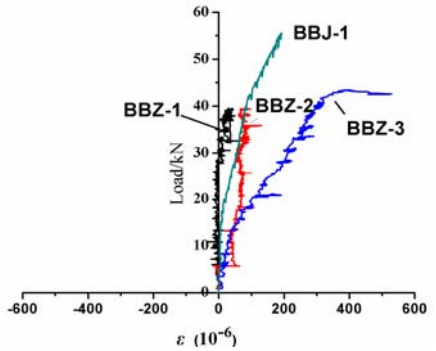

Fig. 10 Load-strain on the top flange of steel sheet

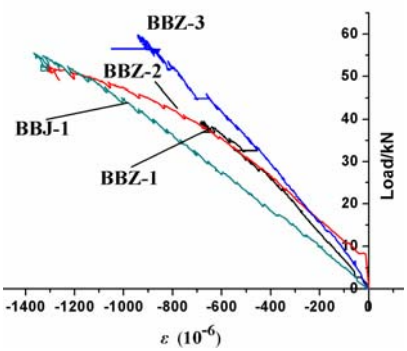

Fig. 11 Load-strain on the surface of concrete slab

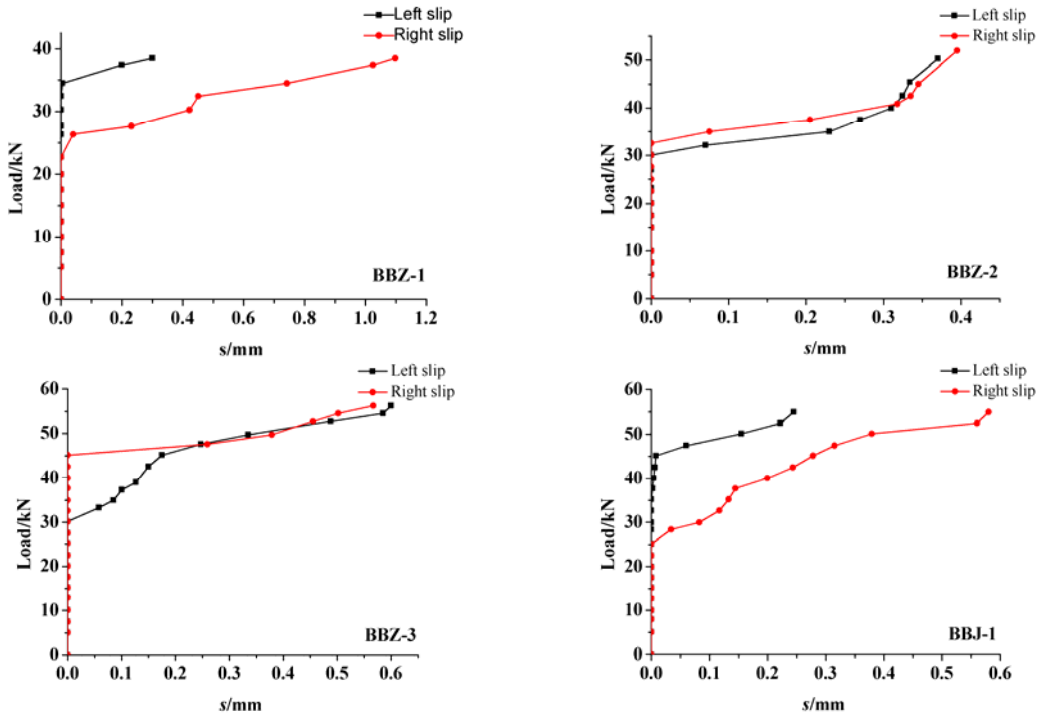

Fig. 12 Load-slip curves of the composite sandwich slabs

the steel deck. As is shown in Fig. 11, the surface of the concrete in the mid-span was under compressive stress and the strains did not exceed the concrete ultimate compressive strain (about 1800×10^{-6}). The results agreed well with phenomena that the mid-span concrete remained being uncracked in the loading history. The cohesive forces between the interface of the profiled steel sheeting and concrete consist of chemical adhesive force, friction, and mechanical interlocking force. Before the slip was observed, the longitudinal shear force was undergone by chemical adhesive force totally. As is shown in Fig. 12, when the load reached approximately 50%～65% P_{max}, the end slip were observed. The major reason is that the different deformation of the concrete

Table 5 The comparison of composite sandwich slabs with normal composite slabs

Ref.	No.	Span/mm	Thickness of steel plate/mm	Failure mode	End slip s_{max} /mm	Shear connectors
This paper	BBZ-1	2400	0.8	Bending failure	1.08	√*
	BBZ-2	2400	0.8	Bending failure	0.31	√
	BBZ-3	2400	0.8	Bending failure	0.6	√
	BBJ-1	2400	0.8	Bending failure	0.25	√
Wang *et al*. (2011)	SP-2a	2400	0.8	Longitudinal shear failure	6	—
		2400	0.8	Longitudinal shear failure	6.5	—

"√*" means with shear connectors;
"—" means without shear connectors

and profiled steel sheeting lead to crushing or shears fracture of cement crystal, which caused failure of chemical adhesive force. After the observation of end slip, friction and mechanical interlocking force started to bear the longitudinal force instead of chemical adhesive force. As the load increased, the end slip grew slowly. The small growth of end slip was mostly the results of shear connectors lied in the shear spans, which restrained the longitudinal movement of the concrete.

Wang *et al*. (2011) conducted normal composite slabs tests and the test specimens were identical as what are studied in this paper. Based on test data presented in Table 5, the normal composite slabs without shear connectors tend to suffer longitudinal shear failure, which belongs to brittle failure; while the composite sandwich slabs with shear connectors lied in the shear span have higher longitudinal shear bearing-capacity. Thus, when the number of shear connectors was set properly, the failure mode of composite sandwich slabs was controlled by bending-bearing capacity.

5. Analysis of sagging bending capacity

5.1 Basic assumption

The calculation for ultimate resistance to sagging bending of a composite sandwich slab is based on the test phenomena and referred to *Euro Code4*. The main assumptions are as follows:

(1) Plane cross-section of the steel deck and concrete parts of a composite section each remain plane;
(2) The tensile strength of concrete is neglected and only the profiled steel sheeting resists the tension force;
(3) Slips between the interface of the steel deck and the concrete are neglected.
(4) Effective area of the steel sheeting is stressed to its yielding strength f_y in tension or compression; the effective area of concrete in compression resists a stress of f_c.
(5) Bending-bearing capacity of the styrofoam material is neglected;

(6) Considering that disparity of rigidity and strength of styrofoam and concrete, additionally styrofoam plate cannot exert restriction effect on concrete, hence the interface between two materials see it as being free.

5.2 Equations of the bend-bearing capacity

Two cases have to be considered according to the position of the plastic neutral axis, when calculating the resistance to sagging bending.

(1) Neutral axis above the steel sheeting, the stress distributions are shown in Fig. 13

$$A_p f_y \le f_c h_c b \tag{1}$$

Where A_p is the area of steel deck cross section, b is the width of the slab, h_c is the depth of concrete above the steel sheet, f_y is the tensile yielding stress of the steel sheet and f_c is the uniaxial compressive strength of the concrete.

Based on the equilibrium of the horizontal forces, the compressive depth of the stress block in the concrete is given by

$$x = A_p f_y / (b f_c) \tag{2}$$

and the sagging bending resistance of a composite sandwich slab is equal to

$$M_u = A_p f_y (d_p - 0.5x) \tag{3}$$

Where d_p is the distance from the top of the slab to the centroid of the effective area of the steel sheet and other parameters are as above.

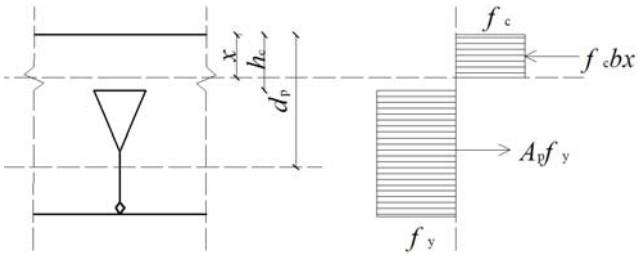

Fig. 13 Stress distribution for sagging bending if the plastic neutral axis is above the sheet

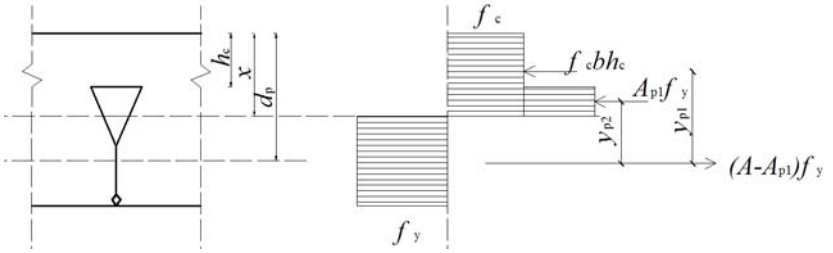

Fig. 14 Stress distribution for sagging bending if the plastic neutral axis is in the steel sheet

(2) Neutral axis within the steel sheeting, the stress distributions are shown in Fig. 14

$$A_p f_y \geq f_c h_c b \tag{4}$$

The concrete in the ribs is neglected for the sack of simplification, because the area of the concrete in the trapezoidal ribs of the steel deck above the neutral axis is of relatively small section and is located near the neutral axis.

Based on the equilibrium of the horizontal forces, the equations are given by

$$f_c h_c b + A_{p1} f_y = (A - A_{p1}) f_y \tag{5}$$

Where A_{p1} is the area of the steel deck above the neutral axis.
and the sagging bending resistance of a composite sandwich slab is equal to

$$M_u = (f_c h_c b y_{p1} + A_{p1} f_y y_{p2}) \tag{6}$$

Where y_{p1}, y_{p2} are the distance from the resultant force of stress under the tensile zone of the steel deck to the resultant force of stress under the compressive zone of the steel deck and the concrete respectively.

Based on the calculated results of Eqs. (1) and (4), the neutral axis for all 4 test specimens were above the steel sheet, when they reached ultimate failure loads. This was consistent with the results that upper flange of the steel sheet were under tensile zone in the loading history, as is shown in Fig. 9. Hence, the resistance moment to sagging bending could be calculated according to Eq. (3). The comparison of test results with calculated results of the sagging bending resistance of the slabs are shown in Table 6. The results showed that the maximum difference of the sagging bending resistance was less than 10% between the calculated results and test results for the specimens with shear screws, while the maximum difference reached 13% of the slab with shear steel bars.

5.3 Influencing factors of the bending-bearing capacity

5.3.1 The depth of the concrete

All other influencing factors being equal, the sagging bending resistance of the composite sandwich slabs increases when the depth of the concrete increases. Comparing among 3 composite sandwich slabs including BBZ-1, BBZ-2 and BBZ-3, with the increase of the concrete depth by 10 mm, the sagging bending resistance increases by 12%. The results indicate that the depth of the

Table 6 The comparison of calculated results with test results

No.	Types of shear connectors	Calculated results	Test results	Calculated results/test results
		M_p (kN·m)	M_{max} (kN·m)	M_{max}/M_p
BBZ-1	Self-drilling screws	12.67	11.86	1.06
BBZ-2	Self-drilling screws	14.42	15.86	0.91
BBZ-3	Self-drilling screws	16.73	18.17	0.92
BBJ-1	Steel bars	14.59	16.67	0.87

concrete is the one important influencing factor, which determines the sagging bending resistance. When the depth of the concrete increases, the internal lever arm of the cross section increases, and then leads to the increase of the resisting moment and high sagging bending resistance of the composite sandwich slabs. However, when the depth of the concrete exceeds certain limit, the sagging bending resistance would not increase any further like the inadequate-reinforced concrete slabs.

5.3.2 The depth of the steel profiled sheet

All other influencing factors being equal, when the depth of the steel profiled sheet increases, the section flexural rigidity of the composite sandwich slabs increases and then leads to the increase of sagging bending resistance. In order to prevent the composite slabs from failure like the over-reinforced concrete slabs and meantime guarantee the economy of the cross-section, the ration of the steel sheet area $\rho = A_p / (bh_o)$ should not exceed ρ_b, where ρ_b is the balanced condition ration: $\rho_b = \beta_1 f_c [\varepsilon_{cu} E_s (h - d_d)] / [f_y d_p (\varepsilon_c + f_y)]$. Where β_1 is the ratio of depth of the compressive stress block to the depth of the neutral axis, ε_{cu} is the ultimate concrete compressive strain, the E_s is elastic modulus of the steel sheet, d_d is the height of the steel sheet.

5.3.3 Shear connectors

The shear screws may enhance the interaction between the steel sheet and the concrete and holistic resistant behavior of the composite sandwich slabs effectively. The maximum end slips reached 0.31 mm and 0.6 mm respectively for the specimens BBZ-2 and BBZ-3, while the end slip for specimen BBZ-1is much larger than them. The thickness of the concrete above the upper flange of the steel sheet is 20 mm. It is the thinner thickness of the concrete for BBZ-1 that leads to the insufficiency of grip strength and the larger end slips. Thus, if the horizontal shear force is only resisted by the adhesion of the steel deck to the concrete without the shear screws, the composite sandwich slabs might suffer longitudinal shear failure. It should be avoided in practical engineering.

The end slip was less than 0.5 mm between the interface of the steel sheet and the concrete for the specimen BBJ-1, when it reached its ultimate load carrying capacity. This indicated that the shear steel bars served to increase the horizontal shear resistance of the composite sandwich slab avoiding the longitudinal shear failure. However, due to its inconvenience of construction and uncontrollable welding quality, the steel bars shear connector should be applied carefully.

In summary, based on the results of the tests, the presence of the self-drilling shear connectors can prevent the composite sandwich slabs from longitudinal shear failure and guarantee the full shear connection.

6. Conclusions

The behavior and load carrying capacity of the re-entrant trough profiled steel sheeting-styrofoam-concrete composite sandwich slabs have been investigated via experiments. Based on the study results, the conclusions can be drawn as follows:

- All of four composite sandwich slab specimens suffer flexural failure and advanced composite action are achieved under static loadings. From initial loading to the final failure, the composite sandwich slab specimens go through three stages: elastic stage, inelastic stage and load declining stage. A re-entrant trough profiled steel sheeting-styrofoam-concrete composite sandwich slab has high sagging bending resistance and good ductility. Therefore,

this slab is worthy of extending to wide use.

- It is advisable to install self-drilling screws as the shear connectors. Self-drilling screws can effectively lessen the end slips between the interface and the vertical uplift displacement, and hence enhance the cooperation of the concrete and steel sheet. However, the steel bar shear connector should be applied carefully because it is hard to guarantee the good welding quality and is inconvenient to install.
- The shear screws can be designed based on elastic method, which can basically prevent the composite sandwich slabs from the bond-slip under the serviceability limit state. The relative slip between the interface of steel deck and concrete can be ignored and thus bending-bearing capacity of slabs can be calculated based on the assumption that full interaction is achieved.
- The deduced equation has a simple form and high computational accuracy for the sagging bending resistance of the re-entrant trough profiled steel sheeting- styrofoam-concrete composite sandwich slabs, and that equation can be used in construction design.

References

Ahn, J.H., Lee, C.G. and Won, J.H. (2010), "Shear resistance of the perfobond-rib shear connector depending on concrete strength and rib arrangement", *J. Constr. Steel Res.*, **66**(10), 1295-1307.

de Andrade, S.A.L., Vellasco, P.C.G.da.S., da Silva, J.G.S. and Takey, T.H. (2004), "Standardized composite slab systems for building constructions", *J. Constr. Steel Res.*, **60**(3-5), 493-524.

EN 1994-1-2 (2003), *Eurocode 4: Design of Composite Steel and Concrete Structures, Part 1.1 General Rules and Rules for Buildings,* European Committee for Standardization, Brussels.

JGJ55-2000 (2000), *Specification for Mix Proportion Design of Ordinary Concrete*, China Architecture and Building Press, Beijing. [in Chinese]

JGJ99-98 (1998), *Technical Specification for Steel Structures of Tall Buildings*, China Architecture and Building Press, Beijing. [in Chinese]

Johnson, R. and Buckby, R. (2004), *Composite Structures of Steel and Concrete*, (2nd Edition), Blackwell Scientific Publications, Oxford, UK.

Kim, H.Y. and Jeong, Y.J. (2010), "Ultimate strength of a steel-concrete composite bridge deck slab with profiled sheeting", *Eng. Struct.*, **32**(2), 534-546.

Maleki, S. and Bagheri, S. (2008a), "Behavior of channel shear connectors, Part I: Experimental study", *J. Constr. Steel Res.*, **64**(12), 1333-1340.

Maleki, S. and Bagheri, S. (2008b), "Behavior of channel shear connectors, Part II: Analytical study", *J. Constr. Steel Res.*, **64**(12), 1341-1348.

Maleki, S. and Mahoutian, M. (2009), "Experimental and analytical study on channel shear connectors in fiber-reinforced concrete", *J. Constr. Steel Res.*, **65**(8-9), 1787-1793.

Porter, M. and Ekberg, Jr. C.E. (1976), "Design recommendations for steel deck floor slabs", *J. Struc. Div.*, ASCE, **102**(ST11), 2121-2136.

Porter, M.L., Ekberg, Jr. C.E. and Greimann, L.F. and Elleby, H.A. (1976), "Shear-Bond analysis of steel-deck-reinforced slabs", *J. Struc. Div.,* ASCE, **102**(ST12), 2255-2268.

Schuster, R.M. and Ekberg, Jr. C.E. (1970), "Commentary on the tentative recommendation of the design of cold-formed steel decking as reinforcement for concrete floor Slabs", Iowa University, Iowa, USA.

Vianna, J.D.C., Costa-Neves, L.F. and Vellasco, P.C.G. (2008), "Structural behaviour of T-Perfobond shear connectors in composite girders: An experimental approach", *Eng. Struct.*, **30**(9), 2381-2391.

Vianna, J.D.C., Costa-Neves, L.F., Vellasco, P.C.G. and de Andrade, S.A.L. (2009), "Experimental assessment of Perfobond and T-Perfobond shear connectors' structural response", *J. Constr. Steel Res.*, **65**(2), 408-421.

Wang, X.T., Luo, G.Q. and Hao, J.P. (2011), "Study on the longitudinal shear behavior of closed profiled steel sheet concrete composite Slab", Xi'an University of Architecture & Technology, (Natural Science Edition), **43**(03), 335-341. [in Chinese]

CC